Alexandria Engineering Journal (2017) xxx, xxx–xxx

HOSTED BY

Alexandria University

Alexandria Engineering Journal

www.elsevier.com/locate/aej
www.sciencedirect.com

ORIGINAL ARTICLE

Impact of thermal radiation on electrical MHD flow of nanofluid over nonlinear stretching sheet with variable thickness

Yahaya Shagaiya Daniel [a], Zainal Abdul Aziz [a,*], Zuhaila Ismail [a], Faisal Salah [b]

[a] UTM Centre for Industrial and Applied Mathematics, Universiti Teknologi Malaysia, 81310 UTM Johor Bahru, Johor, Malaysia
[b] Department of Mathematics, Faculty of Science, University of Kordofan, Elobied 51111, Sudan

Received 13 February 2017; revised 27 June 2017; accepted 10 July 2017

KEYWORDS

MHD nanofluid;
Variable thickness;
Thermal radiation;
Similarity solution;
Viscous dissipation

Abstract The present paper addresses magnetohydrodynamics (MHD) flow of nanofluid towards nonlinear stretched surface with variable thickness in the presence of electric field. The analysis is presented with viscous dissipation, Joule heating, and chemical reaction. Characteristics of heat transfer are analyzed with the electric field and variable thickness phenomenon. The partial differential equations are converted into dimensionless ordinary differential equations by employing suitable transformations. Implicit finite difference scheme is implemented to solve the governing dimensionless problems. Behaviors of several sundry variables on the flow and heat transfer are scrutinized. Skin friction coefficient, the local Nusselt number local Sherwood number are presented and evaluated. It is observed that the skin friction, the rate of heat and mass transfer reduces with a rise in wall thickness. Electric field enhances the nanofluid velocity and temperature but reduced the concentration. Thermal radiation is sensitive to an increase in the nanofluid temperature and thicker thermal boundary layer thickness. Obtained results are also compared with the available data in the limiting case and good agreement is noted.

1. Introduction

The boundary layer flow of an electrical conducting nanofluid toward a stretching sheet has been an active area of research recently. Nanofluid is a fluid produced by a uniform suspension of nano/micro-sized solid particles (metallic/nonmetallic/nanofibers) with a typical size less than 100 nm in a conventional base fluid (liquid). One of these approaches is the addition of small-sized solid particles to the liquid. This method tends to enhance the thermal conductivity of the base fluid approximately twice and the convective heat transfer performance [1–5]. The flow due to stretching boundary has extensive coverage in the extrusion processes involves in plastic and metal industries. Magnetohydrodynamic (MHD) nanofluid is very important in the area of science, engineering, and technology. These fluids are more applicable in the optical modulators, optical grating, tunable optical fiber filters, optical

* Corresponding author.
E-mail addresses: shagaiya12@gmail.com (Y.S. Daniel), zainalaz@utm.my (Z.A. Aziz), zuhaila@utm.my (Z. Ismail), faisal19999@yahoo.com (F. Salah).
Peer review under responsibility of Faculty of Engineering, Alexandria University.

http://dx.doi.org/10.1016/j.aej.2017.07.007

Nomenclature

B_0	magnetic field
B	applied magnetic field
c_f	skin friction coefficient
C_∞	ambient concentration
D_B	Brownian diffusion coefficient
D_T	thermophoresis diffusion coefficient
E_0	electric field factor
E_1	electrical field parameter
E	applied electric field
Ec	Eckert number
f	dimensionless stream function
$\bar{J}$	Joule current
k, k_{nf}	thermal conductivity
k_f, k_p	thermal conductivity of the base fluid and nanoparticle
Le	Lewis number
M	magnetic field parameter
N	buoyancy ratio parameter
Nb	Brownian motion parameter
Nt	thermophoresis parameter
Nu	local Nusselt number
Pr	Prandtl number
q_m	wall mass flux
q_r	radiative heat flux
q_w	wall heat flux
Rd	radiation parameter
Re_x	local Reynolds number
Sh	local Sherwood number
T	temperature of the fluid
T_W	constant temperature at the wall
T_∞	ambient temperature
u, v	velocity component along $x-$ and $y-$ direction
$\bar{V}$	velocity fluid
V_W	wall mass transfer

Greek symbols

α	wall thickness parameter
σ^*	Steffan-Boltzmann constant
σ	electrical conductivity
β_{nf}	volumetric volume expansion coefficient of the nanofluid
η	dimensionless similarity variable
μ	dynamic viscosity of the fluid
υ	kinematic viscosity of the fluid
ρ, ρ_{nf}	density
ρ_p	particle density
$(\rho)_f$	density of the fluid
$(\rho c)_f$	heat capacity of the fluid
$(\rho c)_p$	effective heat capacity of a nanoparticle
ψ	stream function
σ	electrical conductivity
φ	concentration of the fluid
φ_W	nanoparticle volume fraction at the surface
φ_∞	nanoparticle volume fraction at large values of
θ	dimensionless temperature
ϕ	dimensionless concentration
τ	ratio between the effective heat transfer capacity and the heat capacity of the fluid
τ_W	surface shear stress
δ	chemical reaction parameter

Subscripts

∞	condition at the free stream
W	condition at the wall/surface

switches, polymer industry, stretching of plastic materials and metallurgy. The desired quality of finished product strongly depends on the cooling and stretching rates through drawing such strips in an electrically conducting fluid with certain characteristics. Magnetic nanofluid is a unique material that possesses both the magnetic and liquid properties. Most of the physical characteristic of these fluids can be tuned through a varying magnetic field. Mabood et al. [6] solved the problem of convective flow due to a stretching sheet of MHD non-Darcian numerically. The result reveals that increase in the magnetic field tends to reduce the nanofluid movement but enhance the temperature and volume fraction concentration. Magnetic field and suction tend to enhance the wall velocity gradient as result of the study conducted for a flow of heat absorption and radiating fluid due to exponential stretching sheet [7]. Devi et al. [8] solved the problem of thermal conductivity and temperature dependent viscosity impacts on hydrodynamic flow due to slandering stretching material numerically. The result obtained reveals that magnetic field there are more than two regulators which may be manipulated to maintain the optimal heat for the glass injection process to obtain the expected design. Magnetic field retards the flow larger wall thickness reduces temperature and velocity gradient as result of the work conducted by Hayat et al. [9] on a magneto-hydrodynamic two-dimensional flow of Williamson nanofluid due to nonlinear variable thickness surface. The thermal radiation impacts in our industrial and engineering field are enormous. Such that, processes are performed at an extreme high temperature under different non-isothermal conditions and in such circumstance where the convective heat transfer coefficients are lower. The Rosseland approximation is applied to describe the radiative heat flux in the heat convective analysis. The radiative heat transfer is practically applicable in hypersonic flights, nuclear power plants, space vehicles, gas turbines, nuclear reactors, the model of pertinent equipment, etc. Influence of viscous dissipation and thermal radiation plays a key role in cooling and heating processes. They should be maintained as minimum as possible in cooling systems. They found that temperature enhances for more Joule heating. Viscous dissipation and Joule heating strongly enhance the temperature field in the presence of magnetic field [10,11]. More recently, in the area of chemical reaction investigation is to give a mathematical model for the system to predict the reactor performance. A chemical reaction occurs within foreign mass and

Please cite this article in press as: Y.S. Daniel et al., Impact of thermal radiation on electrical MHD flow of nanofluid over nonlinear stretching sheet with variable thickness, Alexandria Eng. J. (2017), http://dx.doi.org/10.1016/j.aej.2017.07.007

fluid, which can be ordered by homogeneous/heterogeneous procedures with effects of variable thicked stretched sheet is studied by [12–14]. Such consideration has several usages in the designs, marine, aeronautical constructions, mechanical and civil engineering. Influence of chemical reaction procedures is seen in earthenware production, nourishment, polymer production etc. The study of heat and mass transfer with chemical reaction is very crucial in chemical and hydrometallurgical industries [15–21]. The concentration of nanoparticle rises with chemical reaction and the degree of the chemical reaction as result of work examined by Makinde et al. [22] on MHD variable viscosity reacting flow due to convectively heating plate with effects of thermophoresis and radiative heat transfer in a porous medium. Analytical solution for flow of magnetohydrodynamic chemically reacting and Radiating Elastico-viscous fluid due to vertical permeable medium for free convection heat and mass transfer [23]. The result reveals that viscous drag on the plate is decreased under the influence of chemical reaction whereas it shows reverse impact with thermal radiation. It was revealed that presence of degenerating chemical reaction cases, the axial velocity and cross flow velocity decreases and both these velocities enhance in the generating chemical reaction. In view of these others related works [24–32].

Thermophoresis is a crucial consequence of the Brownian motion of nanoparticles in fluids with a constant temperature gradient and externally sustained. The heat convection and mass diffusion analysis, that particle dispersion is much and the Brownian force is great when the conventional fluid temperature is higher. For the existence of temperature gradient in the flow region of the suspension, small particles disperse faster in the hotter domain and slower in the colder domain. The collective impact of the dispersion of the nanoparticles is their migration from hotter to a colder region of the fluid domain. The help of temperature gradient, nanoparticles motion on the average against this gradient. This average motion of this nanoparticles is known as thermophoresis. The result obtained shows that thermophoretic and Brownian motion on the mass diffusion is quite reverse. Nanoparticle concentration reduces for higher Brownian motion while it enhances for stronger thermophoretic of the nanofluid which enhances the thermal behavior of the fluid [33–36].

The objective of the present study is motivated by the above-referenced investigation and the vast possible industrial and engineering applications. It has been noticed that the heat transfer work in the past has been mostly dealt with a linearly stretching sheet. Very few studies in this direction are made using a nonlinearly stretching sheet. However, no attempt is yet present for the nonlinear stretching sheet with variable thickness for electrical magnetohydrodynamic (EMHD) boundary layer flow of nanofluid with combined influence of thermal radiation, viscous dissipation, and Joule heating. This work introduces such variable thickness on a nonlinearly stretching sheet (assume that this sheet is sufficiently thin with no induced streamwise pressure gradients) on electrical magnetohydrodynamic (EMHD) boundary layer flow of nanofluid over in the literature. This variable thickness nonlinear stretching sheet has extreme coverage in mechanical, civil, aeronautical structure and marine and designs. The presentation discusses the flow of nanofluid over a nonlinearly stretching sheet with a variable thickness on electrical magnetohydrodynamic (EMHD) in the presence of thermal radiation, viscous dissipation and Joule heating incorporating Brownian motion and thermophoresis in the model. The governing equations are transformed using a set of dimensionless variables and then solved numerically using Keller box method [37]. Graphs of various interesting physical embedded parameters are made using graphical illustration for the velocity, temperature and concentration fields. The physical quantities of interest such as local skin friction coefficient, local Nusselt and Sherwood numbers are computed numerically through tables.

2. Mathematical formulation

Consider a two-dimensional steady electrical magnetohydrodynamic (EMHD) nanofluid over a nonlinearly stretching sheet with variable thickness. The velocity of the stretching sheet is denoted as $U_W(x) = U_0(x+b)^n$, and the surface is taken at $y = A_1(x+b)^{\frac{1-n}{2}}$, in which for $n = 1$ the stretching sheet is of the same thickness. The boundary layer equations of the fluid flow are the composition of the continuity equation, the momentum equation, energy equation and concentration equation, which are formulated based on Maxwell's equation and Ohm's law in the presence of Electrical Magneto-Fluid Dynamics (EMHD). The incompressible flow of viscous fluid in the presence of an applied magnetic field B and electric field E is taken into consideration. The flow is due to stretching of a sheet from a slot through two equal and opposite force and thermally radiative. The magnetic and electric fields obey the Ohm's law define $\bar{J} = \sigma(\bar{E} + \bar{V} \times \bar{B})$ where $\bar{J}$ is the Joule current, σ is the electrical conductivity and $\bar{V}$ represent the fluid velocity. T, φ is the fluid temperature and concentration, the ambient values of temperature and nanoparticle volume fraction attained to a constant value of T_∞ and φ_∞. Magnetic field and the electric field of strength $B(x)\&E(x)$ is applied normal to the flow, such that the Reynolds number is selected small. The induced magnetic field is smaller to the applied magnetic field. Hence the induced magnetic field is absence for small magnetic Reynolds number. We choose the Cartesian coordinate system such that x is chosen along the stretching sheet and y -axis denotes the normal to the stretching sheet, u and v are the velocity components of the fluid in the x and y -direction see Fig. 1. We assumed less temperature gradient within the viscous fluid flow in such a way that T^4 can be expressed as a linear function of

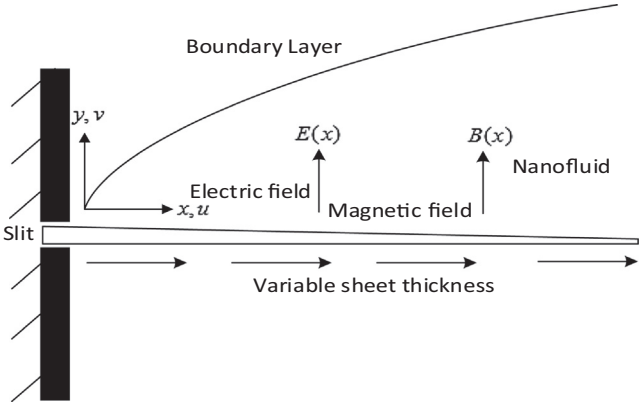

Fig. 1 Physical configuration of the geometry.

temperature. By expanding T^4 using Taylor's series approach about a free stream temperature T_∞. The two-dimensional electrical magnetohydrodynamic (EMHD) boundary layer flow equation of an incompressible electrical conducting nanofluid are given as [5,10,21,23,34,36]:

$$\frac{\partial u}{\partial x}+\frac{\partial v}{\partial y}=0, \tag{1}$$

$$u\frac{\partial u}{\partial x}+v\frac{\partial u}{\partial y}=-\frac{1}{\rho_f}\frac{\partial P}{\partial x}+\nu\left(\frac{\partial^2 u}{\partial x^2}+\frac{\partial^2 u}{\partial y^2}\right)+\frac{\sigma}{\rho_f}(E(x)B(x)-B^2(x)u), \tag{2}$$

$$u\frac{\partial v}{\partial x}+v\frac{\partial v}{\partial y}=-\frac{1}{\rho_f}\frac{\partial P}{\partial y}+\nu\left(\frac{\partial^2 v}{\partial x^2}+\frac{\partial^2 v}{\partial y^2}\right)+\frac{\sigma}{\rho_f}(E(x)B(x)-B^2(x)v), \tag{3}$$

$$u\frac{\partial T}{\partial x}+v\frac{\partial T}{\partial y}=\frac{k}{\rho c_p}\left(\frac{\partial^2 T}{\partial x^2}+\frac{\partial^2 T}{\partial y^2}\right)+\tau\left\{D_B\left(\frac{\partial\varphi}{\partial x}\frac{\partial T}{\partial x}+\frac{\partial\varphi}{\partial y}\frac{\partial T}{\partial y}\right)+\frac{D_T}{T_\infty}\left[\left(\frac{\partial T}{\partial x}\right)^2+\left(\frac{\partial T}{\partial y}\right)^2\right]\right\}+\frac{16\sigma^* T_\infty^3}{3k^*\rho c_p}\frac{\partial^2 T}{\partial y^2}+\frac{\mu}{\rho c_p}\left(\frac{\partial u}{\partial y}\right)^2+\frac{\sigma}{\rho c_p}(uB(x)-E(x))^2, \tag{4}$$

$$u\frac{\partial\varphi}{\partial y}+v\frac{\partial\varphi}{\partial y}=D_B\left(\frac{\partial^2\varphi}{\partial x^2}+\frac{\partial^2\varphi}{\partial y^2}\right)+\frac{D_T}{T_\infty}\left(\frac{\partial^2 T}{\partial x^2}+\frac{\partial^2 T}{\partial y^2}\right)-k^*(\varphi-\varphi_\infty), \tag{5}$$

The magnetic field factor $B(x)=B_0(x+b)^{(n-1)/2}$, σ is the electrical conductivity, $E(x)=E_0(x+b)^{(n-1)/2}$ is the electrical field factor, ν,ρ_f are the kinematic viscosity of the fluid and the fluid density. $k/\rho c_p,\mu,\sigma^*,\rho_{\rho f}$, and ρ_p is the thermal diffusivity, the kinematic viscosity, the Steffan-Boltzmann constant, the density, the fluid density and particles density respectively. We also have $B_0, D_B, D_T, \tau=(\rho c)_p/(\rho c)_f$ which represents the magnetic field, the Brownian diffusion coefficient, the thermophoresis diffusion coefficient, the ratio between the effective heat transfer capacity of the ultrafine nanoparticle material and the heat capacity of the fluid. Follow with the boundary conditions:

$$\begin{aligned}&y=A_1(x+b)^{\frac{(1-n)}{2}},\quad u=U_W(x)=U_0(x+b)^n,\quad v=0,\\&T=T_\infty,\quad \varphi=\varphi_W,\\&y\to\infty:\quad u\to 0,\quad T\to T_\infty,\quad \varphi\to\varphi_\infty,\end{aligned} \tag{6}$$

where c is the stretching sheet constant, b is the stretching rate, and W is the wall natation. To obtain similarity solution of Eqs. (1)–(5) the nondimensional variables are presented as:

$$\begin{aligned}&\psi=\left(\frac{2}{n+1}\nu U_0(x+b)^n\right)^{1/2}F(\xi),\quad \xi=y\left(\frac{n+1}{2\nu}U_0(x+b)^{n-1}\right)^{1/2},\\&\theta(\eta)=(T-T_\infty)/(T_W-T_\infty),\quad \phi(\eta)=(\varphi-\varphi_\infty)/(\varphi_W-\varphi_\infty),\\&u=U_0(x+b)^nF(\xi),\\&v=-\left(\frac{n+1}{2}\nu U_0(x+b)^{n-1}\right)^{1/2}\left(F(\xi)+\xi\frac{n-1}{n+1}F'(\xi)\right),\end{aligned} \tag{7}$$

Using an order magnitude analysis of the y – direction momentum equation (normal to the stretching sheet) applying the normal boundary layer equation as discussed in [21,36]:

$$\begin{aligned}&u\gg v\\&\frac{\partial u}{\partial y}\gg\frac{\partial u}{\partial x},\frac{\partial v}{\partial x},\frac{\partial v}{\partial y}\\&\frac{\partial p}{\partial y}=0.\end{aligned} \tag{8}$$

After employing the boundary layer approximation stated in (8), substitute Eq. (7) into (1)–(3), we obtained the transformed ordinary differential equation as:

$$F'''(\xi)+F(\xi)F''(\xi)-\frac{2n}{n+1}(F'(\xi))^2+M(E_1-F'(\xi))=0 \tag{9}$$

Here $F(\xi)$ is the dimensionless velocity with the following boundary conditions:

$$\begin{aligned}&\xi=0:\quad F(\xi)=\alpha\frac{1-n}{1+n},\quad F'(\xi)=1,\\&\xi\to\infty:\quad F'(\xi)=0\end{aligned} \tag{10}$$

In a similar way, same is applicable to Eqs. (4) and (5). Here $\alpha=A_1\left(\frac{n+1}{2}\frac{U_0}{\nu}\right)^{1/2}$. Taking $F(\xi)=f(\xi-\alpha)=f(\eta)$. The above Eqs. (1)–(9) becomes:

$$f'''(\eta)+f(\eta)f''(\eta)-\frac{2n}{n+1}(f'(\eta))^2+M(E_1-f'(\eta))=0 \tag{11}$$

$$\left(1+\frac{4}{3}Rd\right)\theta''+Pr\left(f\theta'+Nb\phi'\theta'+Nt\theta'^2+Ec(f'')^2+MEc(f'-E_1)^2\right)=0 \tag{12}$$

$$\phi''+\frac{Nt}{Nb}\theta''+Lef\phi'-Le\delta\phi=0 \tag{13}$$

Boundary conditions

$$\begin{aligned}&\eta=0:\quad f(\eta)=\alpha\frac{1-n}{1+n},\quad f'(\eta)=1,\quad \theta(\eta)=1,\quad \phi(\eta)=1\\&\eta\to\infty;\quad f'(\eta)=0,\quad \theta(\eta)=0,\quad \phi(\eta)=0\end{aligned} \tag{14}$$

where α is the wall thickness parameter, $M=2\sigma B_0^2/\rho_f U_0(n+1)$ is the magnetic field parameter, $E_1=E_0/B_0U_0(x+b)^n$ is the electric parameter. $Pr=\mu c_p/k$ is the Prandtl number, $Nb=(\rho c)_p D_B(\varphi_w-\varphi_\infty)/(\rho c)_f\nu$ is the Brownian motion parameter, $Le=\nu/D_B$ is the Lewis number, $Nt=(\rho c)_p D_T(T_w-T_\infty)/(\rho c)_f\nu T_\infty$ is the thermophoresis parameter, $Ec=U_W^2/c_p(T_w-T_\infty)$ is the Eckert number, and $Rd=4\sigma^* T_\infty^3/k^*k$ is the radiation parameter respectively. The Brownian motion is made of a different composition of factor values such as $(\rho c)_p,(\rho c)_f,D_B,\varphi_W,\varphi_\infty,\nu$ and involved of the governing equation under investigation. Here k_f,k_p are the thermal conductivities of the base fluid and nanoparticle, $\delta=2k^*/(n+1)U_0(x+b)^{n-1}$ is the chemical reaction parameter. The c_f is skin friction coefficient defined in terms of shear stress, q_w is the wall heat flux and q_m is the wall mass flux defined as:

$$c_f = \frac{\tau_w}{\rho U_w^2(x)}, q_W = -\left(k + \frac{16\sigma^* T_\infty^3}{3k^*}\right)\frac{\partial T}{\partial y}\Big|_{y=A_1(x+b)^{\frac{(1-n)}{2}}},$$
$$q_m = -D_B \frac{\partial \varphi}{\partial y}\Big|_{y=A_1(x+b)^{\frac{(1-n)}{2}}} \quad (15)$$

where τ_w is the surface shear stress expressed in terms of μ dynamic viscosity of the fluid stretching surface defined as

$$\tau_w = \mu\left(\frac{\partial u}{\partial y}\right)\Big|_{y=A_1(x+b)^{\frac{(1-n)}{2}}},$$
$$Nu_x = (x+b)^{\frac{(1-n)}{2}} q_w / k(T_W - T), Sh_x = \frac{(x+b)^{\frac{(1-n)}{2}} q_m}{D_B(\varphi_w - \varphi_0)}, \quad (16)$$

For the local skin-friction coefficient, Nusselt number and Sherwood number are presented in a non-dimensional form as:

$$Re_x^{1/2} c_{fx} = \sqrt{\frac{1+n}{2}} f''(0),$$
$$Nu_x (Re_x)^{-1/2} = -\left(1 + \frac{4}{3}Rd\right)\sqrt{\frac{1+n}{2}}\theta'(0), \quad (17)$$
$$Sh_x / Re_x^{1/2} = -\sqrt{\frac{1+n}{2}}\phi',$$

Here $Re_x = U_W(x+b)/v$ is the local Reynolds number.

3. Results and discussion

The systems of highly nonlinear ordinary differential Eqs. (11)–(13) with the respective boundary conditions (14) are solved numerically using Keller box method [37] for the velocity, temperature and concentration fields. The computation is repeated until some convergence criterion is satisfied up to the desired accuracy of 10^{-5} level. Comparison with the existing results published by Fang et al. [38] shows a perfect agreement, as presented in Table 1. Table 2 displayed the variation of the skin friction coefficient, local Nusselt and local Sherwood numbers in relation to magnetic field M, thermal radiation Rd, Eckert number Ec, Lewis number Le, Brownian motion Nb, thermophoresis Nt, Prandtl number Pr, power law index n, electric field E_1, chemical reaction δ, and variable thickness α parameters respectively. In this table, numerical values of the skin friction coefficient are presented. The skin friction coefficient increases by increasing $M, \&n$ while it decreases for higher values E_1 and α. Generated values of local Nusselt and Sherwood numbers for different involving parameters are presented in this Table. It is noted that the local Nusselt number decreases for higher values of $M, Rd, Ec, Nb, Nt, Pr, n, E_1$, and α, however, it increases for higher values of Le and δ. For the case of local Sherwood number increases by increasing M, Rd, Ec, Le, Nb, Pr, and E_1 whereas, it decreases for higher values of Nt, n, δ, and α.

We obtained dimensionless velocity, temperature, and nanoparticles concentration distribution for different values of emerging parameters. The case $\alpha = 0.0$ correspond to absence and $\alpha > 0$ corresponds to the presence of wall thickness. The graphical results obtained are displayed in Figs. 2–14 for velocity, temperature, and concentration distribution respectively. Figs. 2–5 demonstrates the velocity graphs for various values of M, E_1, n, and α respectively. Fig. 2a illustrates the influence of the wall thickness and magnetic field parameters on the velocity $f'(\eta)$ in the presence/absence of wall thickness parameter. In this Fig. the velocity profile considerably decreases with an increase in the values of magnetic field parameter when $E_1 = 0.0$ (absence of electric field). It is obvious that the magnetic field dependent on Lorentz force, which is stronger for a larger magnetic field. But due to the absence of electric field, the Lorentz force enhances the frictional force, which acts as a decelerating force that resists the nanofluid flow over a nonlinearly stretching sheet. In the presence of electric field $E_1 = 0.1$ see Fig. 2b as the magnetic field parameter increases, the velocity boundary layer decrease and after some distance away from the wall η, it increases over the non-linear stretching surface intensely. Why because electric field which acts as accelerating body force, accelerate the nanofluid movement over the nonlinear stretching sheet. It leads to an increase in the skin friction at the surface due to increase in magnetic field and decrease for the wall thickness parameter. The momentum boundary layer thickness decreased in the presence

Table 1 Comparison of $-f''(0)$ when $E_1 = M = 0$ for varying values of m.

n	Ref. [38] $-f''(0)$ when $\alpha = 0.25$	Present result	n	Ref. [38] $-f''(0)$ when $\alpha = 0.5$	Present result
10.00	1.1433	1.143316	10.00	1.0603	1.060323
9.00	1.1404	1.140388	9.00	1.0589	1.058914
7.00	1.1323	1.132281	7.00	1.0550	1.055043
5.00	1.1186	1.118587	5.00	1.0486	1.048610
3.00	1.0905	1.090490	3.00	1.0359	1.035867
1.00	1.0000	1.000001	2.00	1.0234	1.023407
0.50	0.9338	0.933828	1.00	1.0000	1.000001
0.00	0.7843	0.784284	0.50	0.9799	0.979948
−1/3	0.5000	0.500000	0.00	0.9576	0.957648
−0.5	0.0833	0.083289	−1/3	1.0000	1.000000
−0.51	0.0385	0.038484	−0.5	1.1667	1.166644
−0.55	−0.1976	−0.197647	−0.51	1.1859	1.185881
−0.60	−0.8503	−0.850207	−0.55	1.2807	1.280697
−0.61	−1.2244	−1.224426	−0.60	1.4522	1.452134
			−0.70	2.0967	2.096621
			−0.80	3.6278	3.627748
			−0.90	8.5457	8.545676

Table 2 Numerical values for Skin friction, local Nusselt and Sherwood numbers $-f''(0), -\theta(0) \& -\phi(0)$ for different values of $M, E_1, n, \& \alpha$.

M	Rd	Ec	Le	Nb	Nt	Pr	n	E_1	δ	α	$c_f Re_x^{1/2}$	$Nu_x Re_x^{-1/2}$	$Sh_x Re_x^{-1/2}$
0.5	0.2	0.1	1.5	0.1	0.1	0.71	1.0	0.1	1.0	0.1	1.121039	0.359880	1.163885
1.0											1.248947	0.358376	1.165497
1.5											1.368476	0.356186	1.166990
2.0											1.479512	0.354990	1.168173
0.1	0.4										1.020145	0.317431	1.175755
	0.6										1.020145	0.291475	1.183204
	0.8										1.020145	0.271860	1.188527
	1.0										1.020145	0.256602	1.192478
	0.2	0.2									1.020145	0.330562	1.183160
		0.4									1.020145	0.285689	1.219829
		0.6									1.020145	0.240804	1.256507
		0.8									1.020145	0.195904	1.293194
		0.1	1.7								1.020145	0.352636	1.251911
			2.0								1.020145	0.352200	1.372828
			2.5								1.020145	0.351656	1.554612
			3.0								1.020145	0.351255	1.718064
			1.5	0.2							1.020145	0.337728	1.195539
				0.3							1.020145	0.323019	1.205617
				0.4							1.020145	0.308853	1.210541
				0.1	0.2						1.020145	0.343668	1.124288
					0.3						1.020145	0.334624	1.093259
					0.4						1.020145	0.325853	1.071096
					0.1	1.2					1.020145	0.471055	1.538188
						2.0					1.020145	0.589626	2.160007
						2.5					1.020145	0.533894	3.420984
						0.71	2.0				1.104931	0.333243	1.152420
							3.0				1.144754	0.323684	1.146165
							4.0				1.167917	0.318043	1.142395
							4.0	1.5			0.921896	0.373888	1.145988
								2.0			0.845503	0.351413	1.161528
								2.5			0.772113	0.312548	1.183351
								1.0	2.0		1.002384	0.378346	1.098864
									3.0		1.002384	0.379084	1.041805
									5.0		1.002384	0.380276	0.943502
									1.0	0.2	0.981554	0.358984	1.114859
										0.5	0.921924	0.305220	1.047845
										0.7	0.884501	0.271721	1.003050
										1.0	0.831738	0.225210	0.936002

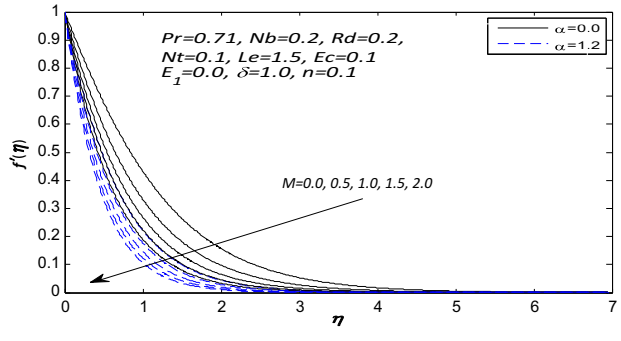

Fig. 2a Influence of M (when $E_1 = 0.0$) on the velocity profile $f'(\eta)$.

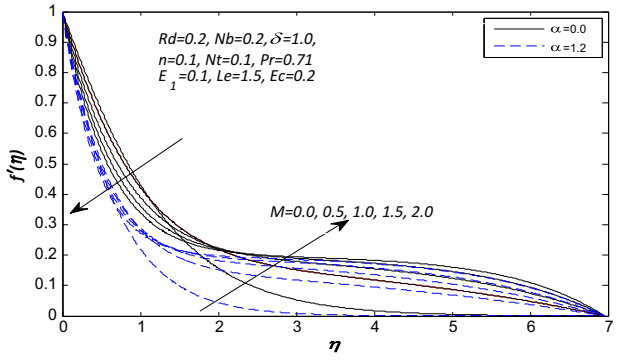

Fig. 2b Influence of M (when $E_1 = 0.1$) on the velocity profile $f'(\eta)$.

of wall thickness parameter for higher values of the magnetic field parameter than in the presence. Influence of wall thickness and electric field parameter on the velocity $f'(\eta)$ is depicted in Fig. 3. It is noticed that the velocity profile of the nanofluid significantly enhanced with an increase in the values of E_1. An increase in wall thickness α results in a decrease in dimensionless velocity field and the momentum

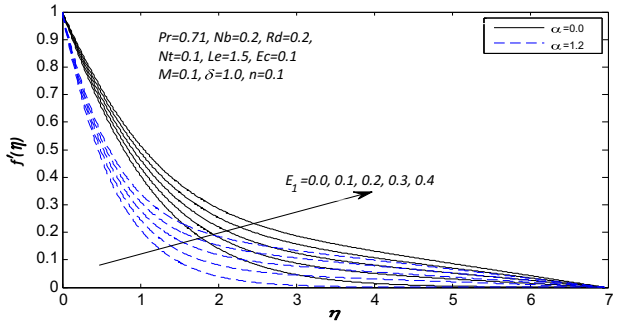

Fig. 3 Influence of E_1 on the velocity profile $f'(\eta)$.

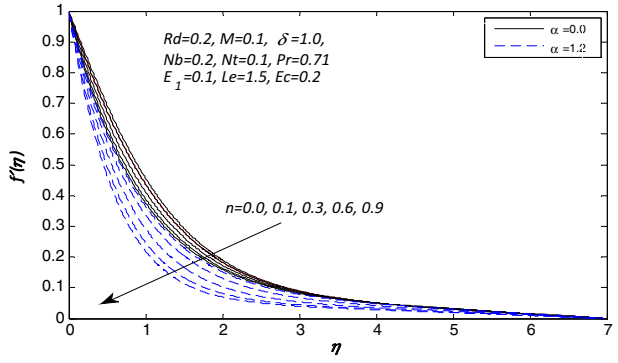

Fig. 4 Influence of n on the velocity profile $f'(\eta)$.

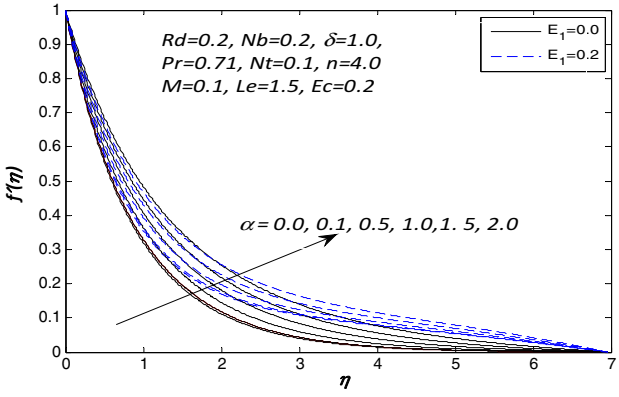

Fig. 5 Influence of α on the velocity profile $f'(\eta)$.

boundary layer thickness. Why because the electric field introduces accelerating body force which acts to the direction of the applied electric field. This body force, known as the Lorentz force, accelerates the boundary layer flow and thickens the momentum boundary layer. Hence it resulted in a reduction in the skin friction at the nonlinear stretching sheet surface. Fig. 4 reveal the influence of wall thickness and nonlinear stretching parameters on the velocity $f'(\eta)$. This dimensionless velocity field clearly shows that it reduced with an increase in nonlinear stretching parameter, which is more pronounced in the presence of wall thickness become thinner, than absence. The momentum boundary layer thickness becomes thinner and the velocity profile reduces. The absolute velocity gradient increases at the surface for the nanofluid flow due to a nonlinearly stretching sheet. In Fig. 5 exposed the impact of wall thickness and electric field parameters on the velocity profile. It is observed that the velocity profile $f'(\eta)$ intensifications with an increase in the values of wall thickness parameter. Due to a presence of electric field parameter E_1, the velocity field decreases and after some distance η away from the wall, it increases near to the nonlinear stretching sheet more. Why because the electric field which behaves as accelerating body force, accelerated the nanofluid flow for some distance away from the wall for large η. The thickness of the momentum boundary layer becomes thicker for higher values of wall thickness parameter and the velocity profile increases monotonically. The skin friction reduces at the surface of the nonlinear stretching sheet for an increase in the values of wall thickness parameter.

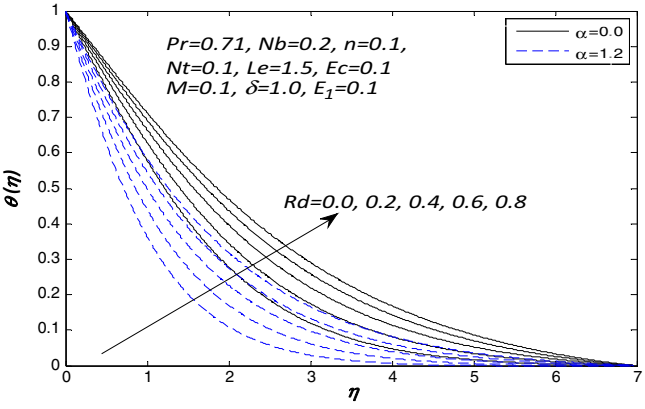

Fig. 6 Influence of Rd on the temperature profile $\theta(\eta)$.

Effects of parameter wall thickness α, thermal radiation Rd, Prandtl number Pr, Eckert number Ec, electric field parameter E_1, and magnetic field parameter M on the temperature profile $\theta(\eta)$ are presented in Figs. 6–10. Fig. 6 indicates that temperature profile $\theta(\eta)$ for combined effects of thermal radiation and wall thickness parameters. It is found that radiation provides enhancement on the fluid temperature as the wall thickness decreased. The rate of heat transfer at the surface reduces for higher thermal radiation effects. Higher temperature and thicker thermal boundary layer thickness associated with larger radiation parameter. Higher values of radiation parameter lead to a low rate of heat transfer at the surface why because the nanofluid temperature is enhanced. The effects of wall thickness and Prandtl number on the dimensionless temperature profile is displayed in Fig. 7. Due to nonlinear stretching flow, the Prandtl number also affects the temperature profile. The temperature $\theta(\eta)$ along the plate decreases with increase in Prandtl number for both presence and absence of wall thickness cases. In both situations as Prandtl number increases, the temperature at every point in the thermal boundary layer reduces as well as the temperature field. This result of an increase of fluid viscosity which leads to a decrease in the fluid temperature as result of high flows of kinetic energy in the distribution. The rate of heat transfer increases at the surface of the stretching sheet for more of Prandtl number effects. Influence of wall thickness and Eckert number on the temperature profile is presented in Fig. 8. It is analyzed that temperature profile increases for high values of Eckert number as the wall thickness reduced. When the values of Eckert number increase,

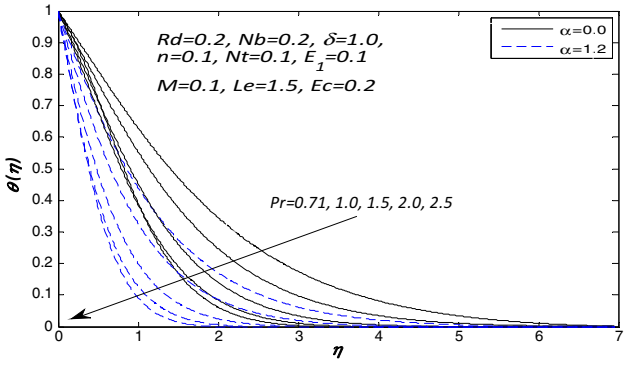

Fig. 7 Influence of Pr on the temperature profile $\theta(\eta)$.

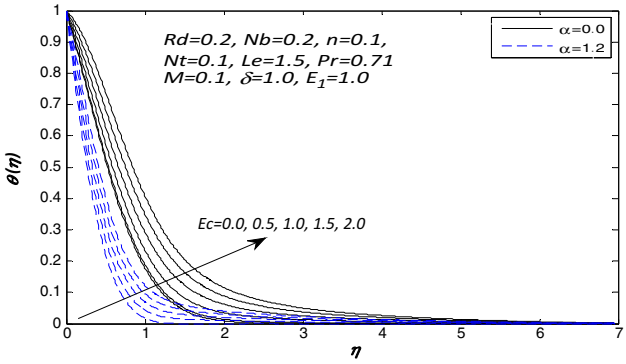

Fig. 8 Influence of Ec on the temperature profile $\theta(\eta)$.

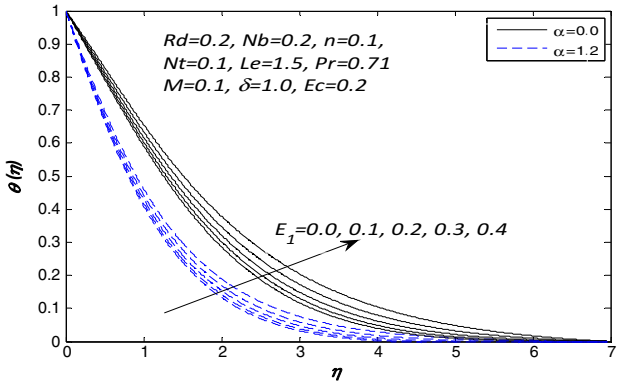

Fig. 9 Influence of E_1 on the temperature profile $\theta(\eta)$.

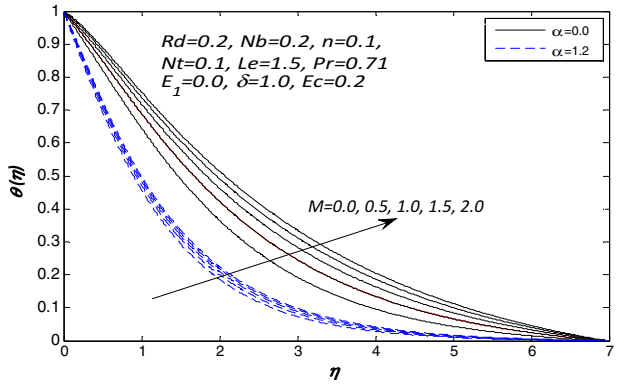

Fig. 10a Influence of M (when $E_1 = 0.0$) on the temperature profile $\theta(\eta)$.

the thermal boundary layer thickness becomes thicker and the temperature field increase. This leads to a low rate of heat transfer at the surface. Fig. 9 portray the effects of wall thickness and electric field parameters on the temperature $\theta(\eta)$ profile. Similar behavior trend with Fig. 3, the rate of heat transfer reduce as electric field and wall thickness rises. The electric field accelerates the fluid temperature due to Lorentz force. This gives rise to the thermal boundary layer thickness and temperature field for both cases of presence and absence of wall thickness parameter. Fig. 10a is plotted to see the change in the temperature $\theta(\eta)$ corresponding to different values of the magnetic field and wall thickness parameters in absence of electric field ($E_1 = 0.0$). We have seen that the temperature and thermal boundary layer thickness are increased monotonically. Lorentz force accelerated the nanofluid resistance that leads to an enhancing in the fluid temperature more in the absence of wall thickness compared to presence. Effects of a magnetic field in the presence of electric field ($E_1 = 0.1$) with wall thickness is displayed in Fig. 10b. It's worth noticing that an increase in the magnetic field tends to reduce the fluid temperature significantly with variable thickness. This is because of the reason that Lorentz force associated with the magnetic field and the presence of an electric field which behave as accelerating body force, leads to decrease in the nanofluid resistance which causes the temperature decreased. The rate of heat transfer reduced with higher values of magnetic field.

To analysis the variations of Brownian motion Nb, thermophoresis Nt, Lewis number Le, chemical reaction δ, electric field E_1 and wall thickness α parameter on the dimensionless concentration $\phi(\eta)$, Figs. 11–15 are sketched. Fig. 11 designates that with the rise of both wall thickness and Brownian motion parameters shows decreasing effects on nanoparticle volume fraction. As the values of Nb and α increase, the solutal boundary layer thickness is decreasing as well as the concentration field. However, the magnitude of mass transfer on the surface of the stretching sheet increases as the values of Brownian motion increase. This is as result of the fact that Brownian motion reduces the fluid concentration which leads to increases in mass transfer rate at the surface. From Fig. 12 demonstrate the effects of combine thermophoresis and wall thickness parameters on concentration profile are monotonic. In the presence of wall thickness, there's high rate of fluid concentration from the wall compared to the presence, distance away from the wall. In a case of the presence more fluid concentration at the nonlinear stretching sheet far away from the wall. The values of thermophoresis parameter increase, the solutal boundary layer thickness becomes thicker and the concentration field increase, as the wall thickness has a reversed effects. Moreover, the magnitude of concentration gradient at the surface of the stretching sheet reduces as the values of thermophoresis. The mass transfer rate at the surface decreases for high values of thermophoresis parameter. The combined impacts of Lewis number and wall thickness parameters are displayed in Fig. 13. As Lewis number and wall thickness parameters increase the concentration profile and the solutal boundary layer thickness decreases. The reason is that mass transfer rate is sensitive to an increase in Lewis number. It also reveals that the Sherwood number at the surface

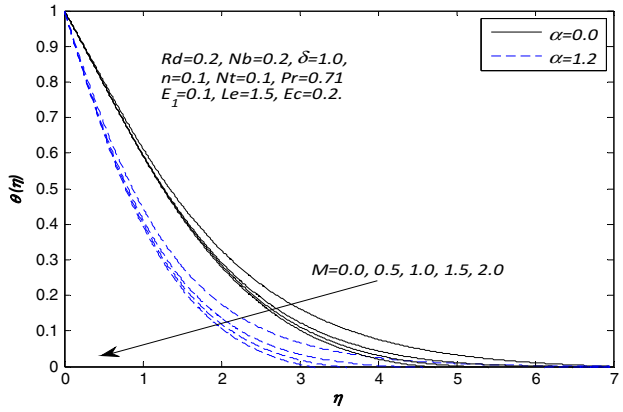

Fig. 10b Influence of M (when $E_1 = 0.1$) on the temperature profile $\theta(\eta)$.

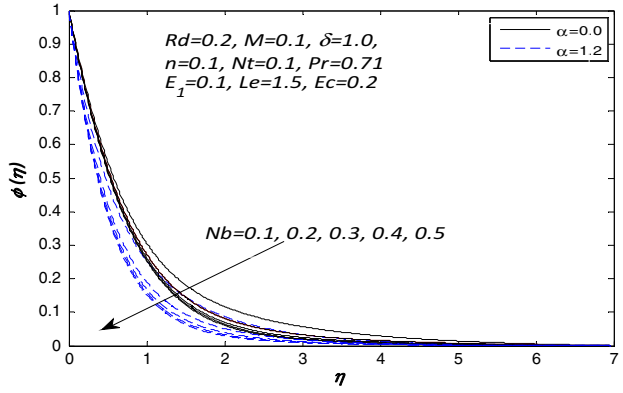

Fig. 11 Influence of Nb on the concentration profile $\phi(\eta)$.

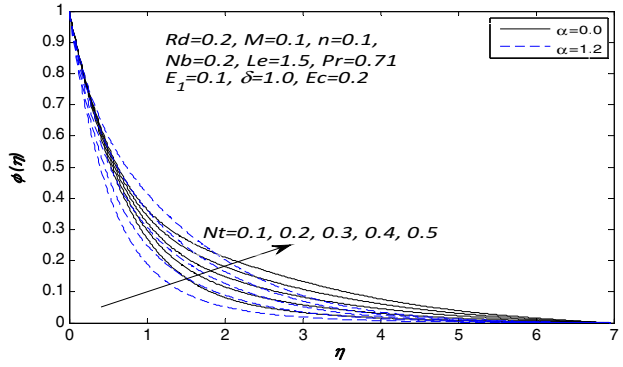

Fig. 12 Influence of Nt on the concentration profile $\phi(\eta)$.

increases. Moreover, the concentration of the nanofluid at the surface reduces more compared to the absence of wall thickness as the values of Lewis number increase. The effects of electric field and wall thickness parameters are depicted in Fig. 14. For higher values of an electric field parameter, the fluid concentration reduces for both cases of presence and absence of wall thickness parameter. The presence of wall thickness parameter reduced the fluid concentration and solutal boundary layer thickness. The rate of mass transfer at the surface increases due to increase in the values of electric field. Fig. 15 reveals the behavior of wall thickness and chemical reaction parameters. It is observed that for an increase in a

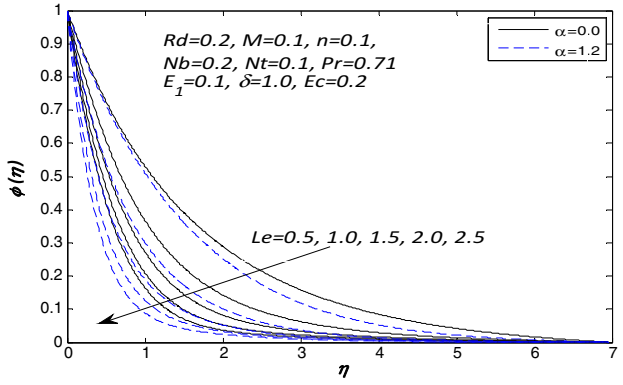

Fig. 13 Influence of Le on the concentration profile $\phi(\eta)$.

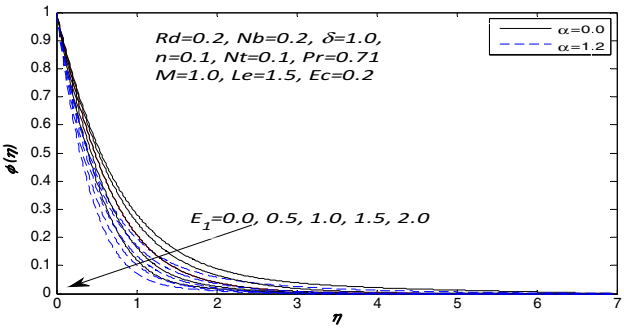

Fig. 14 Influence of E_1 on the concentration profile $\phi(\eta)$.

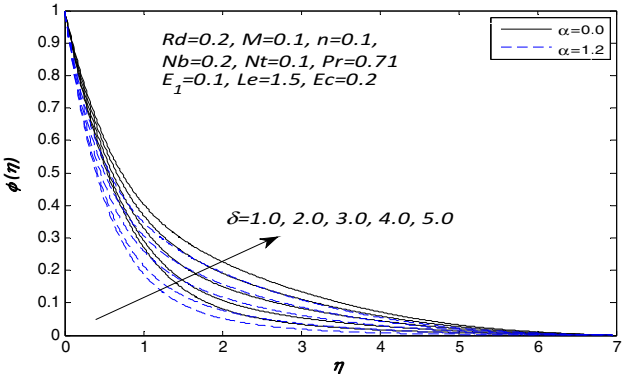

Fig. 15 Influence of δ on the concentration profile $\phi(\eta)$.

chemical reaction, the concentration profile and solutal boundary layer thickness rises. This induces the mass transfer to reduce for an increase for high values of chemical reaction parameter. High values of wall thickness parameter reduce the fluid concentration and solutal boundary layer thickness. The rate of mass transfer reduces at the surface of the stretching sheet for a high rate of chemical reaction.

4. Conclusions

We have studied the combined effects of thermal radiation, chemical reaction, viscous dissipation and Ohmic heating for electrical conducting of nanofluid on boundary layer flow

and heat transfer due to a nonlinearly stretching sheet with a variable thickness in the presence of electric field. A numerical solution has been employed to study steady-state two dimension boundary layer flow and heat transfer due to a nonlinearly stretching sheet with a variable thickness in an electrical conductivity of nanofluid. The effects of various emerging governing parameters on the heat transfer characteristics were examined. The Velocity and temperature profiles, reversed behavior occurred with the effect of magnetic field. Both velocity and temperature fields are increased by increasing the values of an electric field but decrease with concentration. Temperature and thermal boundary layer thickness are increasing functions of thermal radiation, electric field, and Eckert number parameters. Concentration boundary layer thickness decreases with an increase in parameters via Brownian motion, Lewis number and electric field, but increases with an increase in chemical reaction and thermophoresis. Local Nusselt and Sherwood numbers have a reverse effect with Prandtl number, thermal radiation, Eckert number electric and magnetic fields, but increases with Lewis number and decrease with wall thickness and nonlinear stretching sheet parameters. Skin friction, local Nusselt and Sherwood numbers decrease with an increase in values of wall thickness parameter.

Acknowledgments

The authors would like to acknowledge Ministry of Higher Education and Research Management Centre, UTM for the financial support through GUP with vote number 11H90, Flagship grants with vote numbers 03G50 and 03G53 for this research.

References

[1] S.U.S. Choi, Enhancing thermal conductivity of fluids with nanoparticles, ASME-Publications-Fed 231 (1995) 99–106.
[2] Yanhai Lin, Liancun Zheng, Xinxin Zhang, Lianxi Ma, Goong Chen, MHD pseudo-plastic nanofluid unsteady flow and heat transfer in a finite thin film over stretching surface with internal heat generation, Int. J. Heat Mass Transfer 84 (2015) 903–911.
[3] Chaoli Zhang, Liancun Zheng, Xinxin Zhang, Goong Chen, MHD flow and radiation heat transfer of nanofluids in porous media with variable surface heat flux and chemical reaction, Appl. Math. Modelling 39 (1) (2015) 165–181.
[4] Yanhai Lin, Liancun Zheng, Xinxin Zhang, Radiation effects on Marangoni convection flow and heat transfer in pseudo-plastic non-Newtonian nanofluids with variable thermal conductivity, Int. J. Heat Mass Transfer 77 (2014) 708–716.
[5] Liancun Zheng, Chaoli Zhang, Xinxin Zhang, Junhong Zhang, Flow and radiation heat transfer of a nanofluid over a stretching sheet with velocity slip and temperature jump in porous medium, J. Franklin Inst. 350 (5) (2013) 990–1007.
[6] F. Mabood, S.M. Ibrahim, M.M. Rashidi, M.S. Shadloo, Giulio Lorenzini, Non-uniform heat source/sink and Soret effects on MHD non-Darcian convective flow past a stretching sheet in a micropolar fluid with radiation, Int. J. Heat Mass Transfer 93 (2016) 674–682.
[7] Gauri Shanker Seth, Rohit Sharma, Bidyasagar Kumbhakar, Ali J. Chamkha, Hydromagnetic flow of heat absorbing and radiating fluid over exponentially stretching sheet with partial slip and viscous and Joule dissipation, Eng. Comput. 33 (3) (2016) 907–925.
[8] Devi, S.P. Anjali, M. Prakash, Temperature dependent viscosity and thermal conductivity effects on hydromagnetic flow over a slendering stretching sheet, J. Nigerian Math. Soc. 34 (3) (2015) 318–330.
[9] T. Hayat, Gulnaz Bashir, M. Waqas, A. Alsaedi, MHD 2D flow of Williamson nanofluid over a nonlinear variable thicked surface with melting heat transfer, J. Mol. Liquids 223 (2016) 836–844.
[10] Tasawar Hayat, Muhammad Ijaz Khan, Ahmad Alsaedi, Muhammad Imran Khan, Homogeneous-heterogeneous reactions and melting heat transfer effects in the MHD flow by a stretching surface with variable thickness, J. Mol. Liquids 223 (2016) 960–968.
[11] M. Farooq, M. Ijaz Khan, M. Waqas, T. Hayat, A. Alsaedi, M. Imran Khan, MHD stagnation point flow of viscoelastic nanofluid with non-linear radiation effects, J. Mol. Liquids 221 (2016) 1097–1103.
[12] Muhammad Imran Khan, Tasawar Hayat, Muhammad Ijaz Khan, Ahmed Alsaedi, A modified homogeneous-heterogeneous reactions for MHD stagnation flow with viscous dissipation and Joule heating, Int. J. Heat Mass Transfer 113 (2017) 310–317.
[13] T. Hayat, M. Ijaz Khan, M. Farooq, Tabassam Yasmeen, A. Alsaedi, Stagnation point flow with Cattaneo-Christov heat flux and homogeneous-heterogeneous reactions, J. Mol. Liquids 220 (2016) 49–55.
[14] Muhammad Ijaz Khan, Tasawar Hayat, Muhammad Waqas, Muhammad Imran Khan, Ahmed Alsaedi, Impact of heat generation/absorption and homogeneous-heterogeneous reactions on flow of Maxwell fluid, J. Mol. Liquids 233 (2017) 465–470.
[15] Yahaya Shagaiya Daniel, Simon K. Daniel, Effects of buoyancy and thermal radiation on MHD flow over a stretching porous sheet using homotopy analysis method, Alexandria Eng. J. 54 (3) (2015) 705–712.
[16] Muhammad-Ijaz Khan, Tasawar Hayat, Muhammad Waqas, Ahmed Alsaedi, Outcome for chemically reactive aspect in flow of tangent hyperbolic material, J. Mol. Liquids 230 (2017) 143–151.
[17] Yahaya Shagaiya Daniel, Laminar convective boundary layer slip flow over a flat plate using homotopy analysis method, J. Inst. Engineers (India): Series E 97 (2) (2016) 115–121.
[18] T. Hayat, M. Waqas, S.A. Shehzad, A. Alsaedi, A model of solar radiation and Joule heating in magnetohydrodynamic (MHD) convective flow of thixotropic nanofluid, J. Mol. Liquids 215 (2016) 704–710.
[19] T. Hayat, F.M. Mahomed, S. Asghar, Peristaltic flow of a magnetohydrodynamic Johnson-Segalman fluid, Nonlinear Dyn. 40 (4) (2005) 375–385.
[20] T. Hayat, S. Hina, The influence of wall properties on the MHD peristaltic flow of a Maxwell fluid with heat and mass transfer, Nonlinear Anal.: Real World Appl. 11 (4) (2010) 3155–3169.
[21] Yahaya Shagaiya Daniel, Zainal Abdul Aziz, Zuhaila Ismail, Faisal Salah, Effects of thermal radiation, viscous and Joule heating on electrical MHD nanofluid with double stratification, Chin. J. Phys. 55 (3) (2017) 630–651.
[22] O.D. Makinde, W.A. Khan, J.R. Culham, MHD variable viscosity reacting flow over a convectively heated plate in a porous medium with thermophoresis and radiative heat transfer, Int. J. Heat Mass Transfer 93 (2016) 595–604.
[23] Utpal Jyoti Das, Free convection heat and mass transfer flow for magnetohydrodynamic chemically reacting and radiating elastico-viscous fluid past a vertical permeable plate with gravity modulation, Int. J. Appl. Comput. Math. (2016) 1–17.
[24] T. Hayat, M. Ijaz Khan, M. Waqas, A. Alsaedi, Effectiveness of magnetic nanoparticles in radiative flow of Eyring-Powell fluid, J. Mol. Liquids 231 (2017) 126–133.
[25] Tasawar Hayat, Muhammad-Ijaz Khan, Muhammad Waqas, Tabassum Yasmeen, Ahmed Alsaedi, Viscous dissipation effect

in flow of magnetonanofluid with variable properties, J. Mol. Liquids 222 (2016) 47–54.
[26] T. Hayat, M. Ijaz Khan, M. Farooq, A. Alsaedi, T. Yasmeen, Impact of Marangoni convection in the flow of carbon–water nanofluid with thermal radiation, Int. J. Heat Mass Transfer 106 (2017) 810–815.
[27] Tasawar Hayat, Muhammad Tamoor, Muhammad Ijaz Khan, Ahmad Alsaedi, Numerical simulation for nonlinear radiative flow by convective cylinder, Results Phys. 6 (2016) 1031–1035.
[28] M. Tamoor, M. Waqas, M. Ijaz-Khan, Ahmed Alsaedi, T. Hayat, Magnetohydrodynamic flow of Casson fluid over a stretching cylinder, Results Phys. 7 (2017) 498–502.
[29] Muhammad Ijaz Khan, Muhammad Tamoor, Tasawar Hayat, Ahmed Alsaedi, MHD boundary layer thermal slip flow by nonlinearly stretching cylinder with suction/blowing and radiation, Results Phys. 7 (2017) 1207–1211.
[30] M. Khan, K. Maqbool, T. Hayat, Influence of Hall current on the flows of a generalized Oldroyd-B fluid in a porous space, Acta Mech. 184 (1) (2006) 1–13.
[31] T. Hayat, S.A. Shehzad, M. Qasim, S. Obaidat, Radiative flow of Jeffery fluid in a porous medium with power law heat flux and heat source, Nuclear Engineering and Design 243 (2012) 15–19.
[32] T. Hayat, M. Ijaz-Khan, M. Farooq, A. Alsaedi, M. Waqas, Tabassam Yasmeen, Impact of Cattaneo-Christov heat flux model in flow of variable thermal conductivity fluid over a variable thicked surface, Int. J. Heat Mass Transfer 99 (2016) 702–710.
[33] Tasawar Hayat, Muhammad Waqas, Muhammad Ijaz Khan, Ahmed Alsaedi, Analysis of thixotropic nanomaterial in a doubly stratified medium considering magnetic field effects, Int. J. Heat Mass Transfer 102 (2016) 1123–1129.
[34] F. Mabood, W.A. Khan, A.I. Md, Ismail, MHD boundary layer flow and heat transfer of nanofluids over a nonlinear stretching sheet: a numerical study, J. Magn. Magn. Mater. 374 (2015) 569–576.
[35] Yahaya Shagaiya Daniel, Zainal Abdul Aziz, Zuhaila Ismail, Faisal Salah, Entropy analysis in electrical magnetohydrodynamic (MHD) flow of nanofluid with effects of thermal radiation, viscous dissipation, and Chemical reaction, Theor. Appl. Mech. Lett. (2017).
[36] Wubshet Ibrahim, Bandari Shankar, MHD boundary layer flow and heat transfer of a nanofluid past a permeable stretching sheet with velocity, thermal and solutal slip boundary conditions, Comput. Fluids 75 (2013) 1–10.
[37] Tuncer Cebeci, Peter Bradshaw, Physical and Computational Aspects of Convective Heat Transfer, Springer Science & Business Media, 1988.
[38] Tiegang Fang, Ji Zhang, Yongfang Zhong, Boundary layer flow over a stretching sheet with variable thickness, Appl. Math. Comput. 218 (13) (2012) 7241–7252.

Please cite this article in press as: Y.S. Daniel et al., Impact of thermal radiation on electrical MHD flow of nanofluid over nonlinear stretching sheet with variable thickness, Alexandria Eng. J. (2017), http://dx.doi.org/10.1016/j.aej.2017.07.007